Assimilation of Directional Wave Spectra in the Wave Model WAM: An Impact Study from Synthetic Observations in Preparation for the SWIMSAT Satellite Mission

LOTFI AOUF AND JEAN-MICHEL LEFÈVRE

Division of Marine and Oceanography, Météo-France, Toulouse, France

DANIÈLE HAUSER

CETP/IPSL/Université de Versailles Saint Quentin, Vélizy, France

(Manuscript received 18 February 2005, in final form 1 July 2005)

ABSTRACT

Within the framework of the Surface Waves Investigation and Monitoring from Satellite mission (SWIMSAT) proposed to the European Space Agency, an assimilation scheme has been implemented in the Wave Model (WAM) in order to estimate the impact of spectral information on wave prediction. The scheme uses an optimal interpolation and the "spectral partitioning" principle. The synthetic wave spectra are located along a SWIMSAT orbit track and are assimilated in a 4-day-period simulation. Random errors are included to simulate the uncertainties of SWIMSAT instrumentation. The sensitivity of the scheme to background and observational errors and the correlation length is examined. The assimilation impact is investigated for two cases of moderate and large errors of the first guess.

The results show that the assimilation scheme works correctly and the rms errors of significant wave height, mean period, and direction are significantly reduced for both periods of analysis and forecast. The impact on significant wave height is noticeable during the period of analysis and stays efficient for 2-day forecasts. For a large error in the first guess, the impact increases and remains significant for 3-day forecasts.

Statistical analysis of mean wave parameters clearly shows that the use of spectral information yields a better estimate of wave frequency, direction, and low-frequency wave height in comparison with the results based upon assimilation of wave heights only. However, total significant wave height is less sensitive to the addition of spectral information in the assimilation scheme. The use of correlation length depending on the latitude of grid points leads to a better spread of incremental observations and, hence, to better skills in terms of the rms errors of mean wave parameters. The use of several wavelength cutoffs concerning the SWIMSAT synthetic wave spectra suggests that the "assimilation index" of mean wave parameters decreases with the increasing wavelength cutoff.

1. Introduction

The increasing amount of observations of the sea state prompted the wave community to assimilate the available data in numerical wave prediction models. One of the main objectives of using wave observations from satellites is the better prediction of sea states, which has a crucial impact on human activities at sea, such as ship navigation, coastal survey, and protection against high waves generated by storms or hurricanes. Until now most meteorological services that operate numerical wave models were using satellite information based on only the significant wave height (altimeter data). It has been established that this yields an improvement in the prediction of wave height (Lionello et al. 1992; Le Meur et al. 1995). Improvements are still needed, in particular, for long waves (swell), which are relatively poorly predicted by wave models. Present efforts are focused on integrating spectral information describing dominant wave trains of the sea state into assimilation systems. Now, such information can be obtained from in situ measurements (buoys) or from synthetic aperture radar (SAR) observations, such as those from the Advanced Synthetic Aperture Radar (ASAR) instrument on board the European Space Agency's (ESA) *Environmental Satellite* (*ENVISAT*). Constraining a wave model by spectral information related to

Corresponding author address: Dr. Lotfi Aouf, Division of Marine and Oceanography, Météo-France, 42, Ave. Gaspard Coriolis, 31057 Toulouse CEDEX 01, France.
E-mail: lotfi.aouf@meteo.fr

long waves can also contribute to a better understanding of wave propagation and dissipation.

Pioneer works of Hasselmann et al. (1996, 1997) showed that the assimilation in the WAM model of wave spectra retrieved from the "imagettes" of the *European Remote Sensing Satellite-1* (*ERS-1*) SAR instrument improved the retrieval of some mean wave parameters. To decompose the wave spectra into several dominant wave trains, this approach used optimal interpolation and a partitioning principle. Voorrips et al. (1997) implemented a similar scheme adapted for the assimilation of buoy data located in the North Sea. It was shown that the main improvement in the estimation of wave parameters was obtained for swell cases and, in particular, for the low-frequency significant wave height. The use of other data, such as SAR wave spectra, was studied for regional applications by Breivik et al. (1998) in the North Sea and Dunlap et al. (1998) in the North Atlantic area—in the latter for severe storm conditions where a wave height of 14 m was recorded. The products inverted from the SAR data and used in these studies depend upon external information (a wave model first guess), associated with a relatively low sampling (one SAR spectra every 200 km along the satellite track). This could explain the small assimilation impact found in the above studies. Considering an alternative or complementary data sources can reduce this kind of limitation.

The Surface Waves Investigation and Monitoring from Satellite mission, referred to as SWIMSAT, was submitted to the ESA in 2002 and is aimed at measuring the directional spectra of waves from space using real-aperture radar with a low incidence beam (0°–10°) scanning 0°–360°in azimuth (Hauser et al. 2001b). This would allow measuring the directional spectra of ocean waves along the track at scales ranging from 50 km × 50 km to 90 km × 90 km. Moreover, the inverted wave product should provide a minimum detectable wavelength of about 70 m instead of 200 m for SAR, a resolution in direction of 15° after the averaging process is applied, whereas resolution in wavelength is about 10%–20% of the wavelength.

Because SWIMSAT is not planned yet and wave information from SAR data is still difficult to use, and also because this study started well in advance of the *ENVISAT* launch, we have adopted a methodology based on the use of synthetic observations, obtained from WAM model first guess (offline of any operational use of WAM). A separate publication will be devoted in the near future to the assessment of the assimilation scheme with real *ENVISAT* SAR data.

The main objectives of the present study are, on the one hand, to carry out sensitivity studies on the impact of assimilation, in preparation of the characteristics of SWIMSAT and, on the other hand, to prepare an operational scheme for assimilation of spectral information in operational wave models. Sensitivity studies include a comparison between the assimilation of spectral information and the assimilation of wave heights only, as it already exists in operational models for the assimilation of altimeter data.

The paper is organized as follows. Section 2 briefly describes the assimilation system, which includes the wave model, the optimal interpolation method, and the partitioning principle. Then in section 3, we first discuss the methodology of simulation and the test runs developed for the impact studies. In the second part of section 3, the results of several sensitivity cases of observational and first-guess errors (spectral versus nonspectral), correlation length, and wavelength cutoff, are presented. Finally, in section 4 the principal conclusions of our investigation and comments on future works are presented.

2. Methodology

a. Wave model

The wave model used in this study is the third-generation wave model WAM cycle 4. The reader is reminded that the wave model integrates explicitly the wave energy density equation. The physics of the model consists in expressing the spatial and temporal variation of the wave energy spectrum with external forces of the dynamic system. These forces can induce the generation and dissipation of the waves through wind input, white cap dissipation, energy transfer induced by nonlinear quadruplet interactions, and bottom dissipation [for more details see Günther et al. (1992) and Komen et al. (1994)]. In this study, the wave model WAM cycle 4 was implemented at a global scale covering 80°N–80°S on a regular latitude–longitude grid, at a resolution of 1° latitude by 1° longitude, and the directional wave spectrum was discretized at a resolution of 24 directions, steps of 15°, and 25 frequencies ranging from 0.04 to 0.41 Hz.

b. Assimilation system

The system is based on a combination of the wave model nowcast (background field) and the observations; this generates an analyzed model state. The directional wave spectra are assimilated simultaneously in a multi-time-level scheme over an "assimilation window" of 3 h. The assimilation scheme consists of using an optimal interpolation method applied to mean wave parameters (total energy and wavenumber components of) of each wave train composing the wave spectrum (Voorrips et al. 1997). The partitioning concept is applied to decompose the wave spectrum into a limited number of distinct wave systems (partitions) as, for example, swell generated by storms or wind waves generated by local wind. They are classified and can be identified in observed and modeled wave spectra. Up to four partitions (wave trains) are considered in the scheme.

The first step of the algorithm is to compute the model forecast, which is then interpolated to the observation locations. The second step is to compute the difference between the first-guess and observed parameters, which are called "innovations" or observational increments. Finally, the analyzed field is cast as the sum of the background field and the field of innovations weighted by optimal weights, which are prescribed. The choice of the optimal weights is based on prior estimation of forecast and observation error variances (see below). In summary, the optimal analyzed mean wave parameters are expressed as follows (Kalnay 2002):

$$X^a = X^b + \sum_{i=1}^{N} W_i (X_i^o - \mathbf{H} X_i^b), \tag{1}$$

where X^a and X^b represent the analyzed and first-guess mean wave parameters (total energy and wavenumber components) at each model grid point, respectively. The upper index o (b) stands for observations (first guess), while N is the number of observations affecting model grid points. Here $\mathbf{H}$ is the observation operator that performs the necessary transformation from model space to observation space. The weights assigned to the observations are chosen as follows:

$$W = \mathbf{PH}^{\mathrm{T}}[\mathbf{HPH}^{\mathrm{T}} + \mathbf{R}]^{-1}, \tag{2}$$

where $\mathbf{P}$ and $\mathbf{R}$ are, respectively, the forecast and the observation error covariance matrices. The upper index T means the transpose matrix. The main assumption in the scheme concerns the correlation model, which follows a simple Gaussian form. Therefore, by considering the background error homogeneous and isotropic, we expressed $\mathbf{P}$ and $\mathbf{R}$ as follows:

$$\mathbf{P} = \sigma_b^i \sigma_b^j \exp\left[-\left(\frac{d_{ij}}{\lambda_c}\right)^{1.5}\right] \quad \text{and} \tag{3}$$

$$\mathbf{R} = \sigma_o^2, \tag{4}$$

where i and j are, respectively, the model grid points; d is the distance from the observation location to the grid point; and λ_c is the correlation length. Beyond a threshold distance of influence, which is specified in the assimilation parameters [see section 3a(3)], the model grid points are not affected by the observations. The observation errors are generally assumed to be spatially uncorrelated and, therefore, $\mathbf{R}$ is simplified to a diagonal matrix. In our study, the truth is known; then the background error, which is the difference between the first guess and the truth, can be directly computed. More details will be given on the methodology of the simulation in section 3a. Additional simplification consists in normalizing $\mathbf{P}$ and $\mathbf{R}$ [Eqs. (3)–(4) by the background error, which is specified later in the methodology of simulation (see section 3a)]. Consequently, the relative error, which is by definition the ratio between observation and background error variances (σ_o^2/σ_b^2), becomes a key parameter to give more or less weight to the observations. Several tests run with different relative errors are discussed in section 3b. This tuning process leads to the optimal use of the assimilation scheme.

In practice, in order to avoid numerical errors induced by poor conditioning of the error covariance matrix, we computed this later for boxes, where each one contains a limited number of observation (up to six) and affected grid points. The most difficult part of the assimilation scheme is the cross-assignment of each partition of the observed wave spectrum to the equivalent partition of the first-guess wave spectrum. With this aim, a criterion given by Hasselmann et al. (1997) is used. It consists in computing a "normalized" distance in the spectral space (k_x, k_y) between the mean wave numbers of partitions, as follows:

$$\delta = \frac{(\bar{k}_x^b - \bar{k}_x^o)^2 + (\bar{k}_y^b - \bar{k}_y^o)^2}{(\bar{k}_x^{b2} + \bar{k}_x^{o2}) + (\bar{k}_y^{b2} + \bar{k}_y^{o2})}, \tag{5}$$

where superscripts b and o refer to modeled (background) and observed partitions, respectively, while the overbars indicate the mean value over the wave system (partition). When the estimated distance is less than an assumed threshold value, the partitions are then cross-assigned and are then ready for the optimal interpolation (OI) procedure. Otherwise, the first-guess wave train remains unchanged: The smaller the threshold value, the more restrictive the selection of observed partitions. Note that the maximum value of the cross-assignment distance is 2.

To reconstruct the analyzed wave spectrum, the first-guess partitions are rotated and stretched to match the mean energy, mean direction, and mean frequency of the analyzed partitions. Afterward, the partitions are superimposed to derive a combined wave spectrum. To eliminate gaps between the partitions, a biparabolic interpolation is then applied. For wind sea partitions the driving wind velocity is corrected by using empirical growth law relations (Lionello et al. 1992; Voorrips et

TABLE 1. Description of baseline wave model runs with no assimilation.

Run A	WAM driven by analyzed wind fields without assimilation (truth and perfect observations)
Run B	WAM driven by analyzed wind fields with random errors to simulate the instrumental errors of type 1(see Table 2); no assimilation
Run C	WAM driven by moderate wind field perturbations to simulate moderate first-guess errors; no assimilation
Run D	WAM driven by strong wind field perturbations to simulate large first-guess errors; no assimilation
Run E	As for run B but with simulated instrumental errors of type 2; see Table 2

al. 1997). The wind field is then updated and used to drive the wave model for the following time step.

c. *Assimilation of wave height only*

To evaluate the contribution of assimilating spectral characteristics of waves, it is necessary to make a comparison with the one obtained when assimilating wave height only, as for altimeter data. In this case we do not need a partitioning concept, and the assimilation scheme, which was developed by Lionello et al. (1992), consists in applying an optimal interpolation on the significant wave heights and the stress at the sea surface (from wind speed at 10 m). After separation of the wind sea and swell parts of the wave spectrum, the analyzed parameters (significant wave height and friction velocity) are used to construct an analyzed wind sea spectrum. Then the analyzed wave spectrum can be written as follows:

$$F^a(f, \theta) = AF^b(Bf, \theta), \tag{6}$$

where superscripts a and b stand for analyzed and first guess and f and θ are frequency and direction of the waves. Parameters A and B are computed by using empirical power law relations for growing wind waves, which assumes that dimensionless significant wave height, mean frequency of wind sea, and local wind speed are related (Hasselmann et al. 1997).

3. Impact studies

a. *Methodology of simulation*

1) SYNTHETIC OBSERVATIONS AND ASSOCIATED ERRORS

Synthetic observations used in our experiments were generated as follows. To simulate observations, we first run the WAM driven by wind field analyses from the European Centre for Medium-Range Weather Forecasts (ECMWF) atmospheric model (run A in the following, see Table 1). The modeled directional wave spectra selected at the observation locations are considered to be "perfect" synthetic SWIMSAT wave spectra. The corresponding wave parameters are called the "truth." To take into account that any real observation is associated with instrumental errors, not spatially correlated, we added random errors of Gaussian type in the analyzed wind fields used to generate the synthetic wave field considered as observations. Note that the wind vector is perturbed independently at each single location and time step. Furthermore, a small bias is added to the forcing winds to ensure unbiased mean wave parameters, and the choice of 0.25 m s^{-1} satisfies well this condition. Thus, for the first case of instrumental error, a bias of 0.25 m s^{-1} and a standard deviation of 1 m s^{-1} have been introduced in the analyzed wind field (run B below and in Table 1). The root-mean square (rms) of the difference between outputs of runs A and B corresponds to the prescribed rms error due to instrumental uncertainties. It corresponds to 0.09 m for significant wave height, 0.3 s for the mean period, 8.5° for the propagation direction, and 0.007 m^{-1} for the wavenumber (see also Table 2). This corresponds to a rough estimate of the SWIMSAT instrumental errors, which were estimated (see Hauser et al. 2001a) to be approximately 10% of the mean value for significant wave height and mean period, and 15° for the propagation direction. In other respects, a second set of synthetic observations is computed in order to study the effect of using larger observation errors. The second case of instrumental error uses the same technique as in run B, but with a larger standard deviation of 1.3 m s^{-1} (run E below and in Table 1). For this case, the instrumental uncertainties increases to 0.14 m for significant wave height, 0.4 s for the mean period, 10.6° for the propagation direction, and 0.01 m^{-1} for the wavenumber (see also Table 2).

2) FIRST GUESS

For generating the first-guess wave field, the WAM model was run for the same period as for run A but with a forecast wind field instead of wind analyses to simulate errors on the wave model first guess. Two cases of moderate and strong wind perturbations, which induce different errors on the first-guess wave field, were tested. In the first case, 3-day forecast winds are used (run C below and in Table 1), whereas for the second case 4-day forecast winds with an additional

TABLE 2. Mean value of instrumental rms errors prescribed on wave parameters (significant wave height, mean period, mean direction of wave propagation, and wavenumber) at observation locations. SWH: significant wave height, T: wave period, θ: wave direction, and k: wavenumber.

	Instrumental error 1		Instrumental error 2	
	Rms error	Mean value	Rms error	Mean value
SWH (m)	0.09	2.4	0.14	2.6
T (s)	0.3	8.5	0.4	8.6
θ (°)	8.4	173.2	10.6	174.4
k (m^{-1})	0.007	0.065	0.01	0.064

Gaussian type error of standard deviation of 0.7 m s^{-1} have been considered (run D below and in Table 1). The rms difference between the analyzed and disturbed wind fields is shown in Fig. 1 for the two cases of perturbation, as a function of time. The rms errors have mean values of 2.1 and 2.7 m s^{-1} for a moderate and strong perturbation, respectively. Systematic analyses through comparison of analyzed ECMWF winds with buoy observations from December 1996 to December 1999 have shown that the rms error for the ECMWF wind fields is typically 1.4 m s^{-1} (Bidlot et al. 2000). Therefore, our prescribed first-guess errors on wind speed are larger than for the ECMWF wind analyses, but are relatively similar to the error of typical wave forecasts from operational models. By comparing outputs from runs C and D to the truth (run A), we computed a mean estimate of background errors over all sea points. For run C, the mean value of the standard deviation for significant wave height and mean period are 0.36 m and 0.85 s. These valuesincrease to 0.5 m and 0.90 s for the case of run D. The estimated mean errors on the mean wavenumber for runs C and D are about 0.012 and 0.02 m^{-1}, respectively.

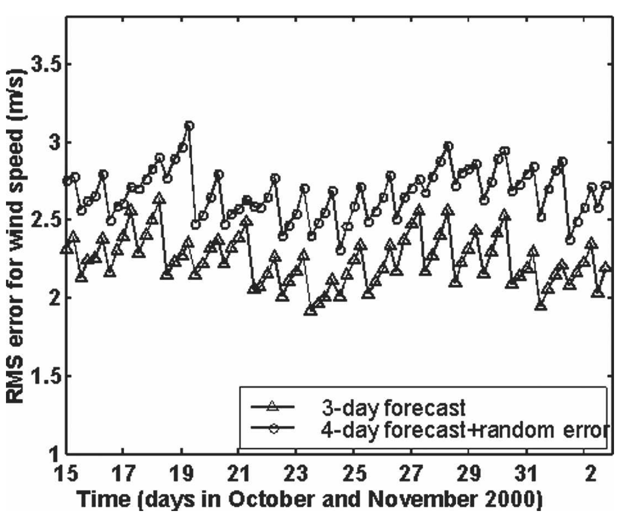

FIG. 1. Time series of the rms error of wind speed (at 10 m above sea surface). Circles and triangles indicate the 4-day forecast ECMWF wind fields with additional random error (standard deviation of 0.7 m s^{-1}) and the 3-day forecast ECMWF wind fields, respectively.

3) CHOICE OF PERIODS AND PRESENTATION OF SENSITIVITY EXPERIMENTS

The assimilation procedure considers the following steps. First, the wave model WAM is run for a one-week period to get a well-established sea state. Thereafter, the assimilation is carried out for a period of 4 days, from 0000 UTC 22 October 2000 until 0000 UTC 26 October 2000. After this date the period of forecast is considered to estimate for how long the assimilation stays efficient (or "keeps an impact"). The assimilation time step is 3 h and the observation locations follow an orbit track for SWIMSAT chosen here with a repeat cycle of approximately 17 days.

Several tests of the assimilation have been performed (see also Table 3) with various assumptions on observation errors, first-guess errors, and parameters of the optimal interpolation procedure. In the first case (run 1a), errors in observations are considered as described above, errors in the first guess correspond to case C in Table 1, and the parameters of the optimal interpolation are relative error (σ_o/σ_b) of 0.6, correlation length of 250 km, cross-assignment threshold of 2, and distance of influence of 600 km. Runs 1b, 1c, and 1d are similar to run 1a, but with relative errors of 1, 0.5, and 0.3. Run 1e uses separate error covariance matrices for significant wave height and wavenumber components, with corresponding relative errors of 0.3 and 0.6, respectively. These latter values chosen for the relative errors in run 1e were estimated by comparing the standard deviation between runs B and C. In run 2, the same parameters as in run 1a are assumed for instrumental errors and first-guess errors, but the assimilation is performed on wave height only (as in the case of altimeter data). Run 3 is similar to run 1a, but with a larger error in the first guess (case D in Table 1); consequently, this leads to using a mean relative error of 0.3 for an optimal computation of weights. Run 4 uses a second case of synthetic observations with an instrumental error corresponding to case E in Table 1, and errors in first guess as in run 1a. To compute optimally the weights for run 4, a mean relative error of 0.6 has been used. The correlation length used in runs 1–4 is a constant value of 250 km. In run 5 we investigated the effect of using a correlation length depending upon latitudes of the grid points and observation locations [see section 3b(5)]. Runs 6, 7, and 8 examine the effects of using wavelength cutoffs of 70, 155, and 240 m, respec-

TABLE 3. List of the performed assimilation runs.

Run 1a	WAM case C in Table 1 (moderate first-guess errors), with assimilation of synthetic wave spectra with moderate instrumental errors (type 1 in Table 2); relative error of 0.6, correlation length of 250 km, cross-assignment threshold of 2, and distance of influence of 600 km
Run 1b	Same as 1a but with a relative error of 1
Run 1c	Same as 1a but with a relative error of 0.5
Run 1d	Same as 1a but with a relative error of 0.3
Run 1e	Same as 1a but with two separate covariance matrices with relative errors of 0.3 and 0.6 for significant wave height and wavenumber, respectively
Run 2	Same as 1a but with assimilation of wave height only
Run 3	Same as 1a but for WAM case D (large first-guess errors) and an optimal mean relative error of 0.3
Run 4	Same as 1a but with assimilation of synthetic wave spectra with large instrumental errors (type 2 of Table 2); the mean relative error is of 0.6 for an optimal run
Run 5	Same as 1a but with correlation length computed from relation (9)
Run 6	Same as 1a but with wavelength cutoff of 70 m
Run 7	Same as 1a but with wavelength cutoff of 155 m
Run 8	Same as 1a but with wavelength cutoff of 240 m

tively, for SWIMSAT synthetic wave spectra. For these runs, we used similar assumptions on the first-guess and observation errors, as well as optimal interpolation, as in run 1a. The threshold distance for cross-assignment between first-guess and observed mean partitions is fixed for all runs to the maximum value of 2.

b. Results

To assess the impact of synthetic SWIMSAT data on wave parameters during the periods of analysis and forecast, we now compare model output from different runs mentioned in Tables 1 and 3. In the following, the impact of assimilation will be discussed by comparing the fields of wave parameters (wave height, mean frequency, mean direction of propagation) in different simulation conditions. An additional parameter referred to as low-frequency wave height is also considered. It is the significant wave height computed over a limited range of wave frequency (see appendix A). This parameter can be easily computed from most remote sensing measurement systems (SAR or SWIMSAT), and has the advantage of having a correlation time larger than the windsea wave height. In addition we have defined a statistical parameter of immediate relevance called the assimilation index, which is mainly used in the discussion of the results. It is defined as the percentage of reduction with regard to the root-mean-square errors of the wave parameters (see appendix B). The closer to 100% the index value is, the closer to the observations the analyzed wave parameters are; then the better the assimilation skill. On the contrary, a negative value means that the assimilation degrades the first guess.

In the following, two types of impact are discussed in order to provide a relevant description of the assimilation study. The first one consists of comparing model output of the assimilation tests (Table 3) to the observed parameters obtained from run A (truth). This impact evaluates the efficiency of the assimilation scheme. Herein we called it assimilation skill with respect to observation. The second impact is based on a comparison between model outputs with and without assimilation (runs 1a and 2 compared to run C; run 3 compared to run D). This shows how large the difference is on wave parameters induced by the assimilation. We refer to what follows as assimilation skill with respect to no assimilation case.

1) SENSITIVITY TO THE CHOICE OF THE RELATIVE ERROR (OBSERVATION–FIRST GUESS)

As mentioned in section 2b and because of the assumption of using the correlation model given by relation (3), much attention is focused on the choice of relative error that will induce an optimal use of the assimilation scheme. Generally, it is difficult to estimate the observation and background errors; for this reason the tuning process consists of using, at first attempt, a relative error of 1, which means that background and observation errors are equal. Thereafter, we perform assimilation runs by decreasing the relative error until we obtain the best weights for correcting the wave parameters. By comparing mean values of the standard deviations from runs B and C, we find that, for our simulations, the relative errors between background and observation are not the same as the significant wave height and wavenumber: about 0.3 for the significant wave height and 0.6 for the wavenumber. However, to simplify the problem, we first consider a single error covariance matrix for all assimilated wave parameters. This method is used in runs 1a, 1b, 1c, and 1d,

TABLE 4. Mean value of the assimilation index, computed over all sea points, for various relative errors (ratio of the rms error of observations to the rms error of first guess) during the period of analysis and forecast (limited to 2 days). AVAI: average value of the assimilation index, SWH: significant wave height, and f_m: mean wave frequency.

		AVAI (%)	
	Relative error	Analysis	Forecast (2 days)
SWH	1	11.1	3.1
	0.6	12.2	3.6
	0.3 and 0.6	12.3	3.7
	0.5	12	3.5
	0.3	10	3.2
f_m	1	10.8	6.8
	0.6	12.2	7.8
	0.3 and 0.6	12.3	7.7
	0.5	12.1	7.7
	0.3	11.6	6.5

which are associated, respectively, with relative errors of 0.6, 1, 0.5, and 0.3. In addition, to take into account the difference in the relative errors for wave height and wavenumber, we consider in run 1e distinct covariance matrices for each wave parameter with the appropriate relative errors of 0.3 for the significant wave height and 0.6 for the wavenumber.

Table 4 gives mean values of assimilation indexes for significant wave height and mean frequency during the periods of analysis and forecast, for runs 1a–e. Better skill with respect to observations is obtained for runs 1a and 1e. These runs are then the most appropriate for an optimal use of the correlation model given by relation (3). The assimilation index is improved by more than 2% in comparison with the case of relative error of 1 (run 1b). As for the case of relative error of 0.5 (run 1c), the mean value of the assimilation index decreases slightly in comparison with runs 1a and 1e. In the cases for runs 1c and 1d, we found that giving more weights to the observations induces more rejection of the observations from the analysis. The case of a single covariance matrix with a relative error of 0.3 (run 1d) gives the lowest mean assimilation index for both significant wave height and mean frequency of waves in comparison with the other test runs.

In the following, we use a single covariance matrix with a relative error of 0.6 because this agrees with the optimal values of run 1e and requires less CPU time.

2) Spectral versus nonspectral assimilation

When spectral data are assimilated, the impact with respect to the "no assimilation case" during the 4-day period of assimilation (difference between runs 1a and C) is significant: it reaches 2 m in some locations (Fig. 2a). The largest impacts are located in the Southern Hemisphere for the latitude band from 40° to 60°S where high winds are dominant. Figure 2a also shows that the analyzed wave field "keeps memory" of the previous assimilations (signature visible along other orbit tracks). A strong impact of assimilation is also observed for the mean wave period (Fig. 3a), with a maximum impact of more than 4 s in the northwestern part of the Pacific Ocean and in the Southern Hemisphere. Table 5 presents the assimilation index, and the correlation between the modeled and observed wave parameters calculated over all observation locations. The assimilation index—calculated here as the mean value over the observation points—is 48%, 29%, and 36% for the significant wave height, mean wave frequency, and direction, respectively. This shows that the assimilation is quite "efficient" and that the best efficiency is for wave height (and then for direction). Furthermore, the correlation between modeled and observed wave parameters is clearly improved after the assimilation of synthetic wave spectra.

The same analysis for the forecast period indicates that the assimilation impact on significant wave height with respect to the "no assimilation case" remains considerable (Figs. 2b and 2c): 1 day after the end of assimilation it is still more than 0.6 m in the northeast and southern Pacific Ocean, and also in the latitude band of 0°–20°N in the Atlantic Ocean. After 2 days of forecast, the impact decreases progressively and reaches less than 0.3 m, mainly located in the southeast and southwest Pacific Ocean (Fig. 2c). For the mean wave period, the same trend is found as for the significant wave height: 1 day after the assimilation period the impact reaches more than 1.5 s, as illustrated in Fig. 3b. The largest impact is located in the intertropical region, in the southwest Pacific Ocean and also close to southwest coast of Africa. Although after 2 days of forecast, Fig. 3c shows that the impact on mean wave period is still estimated at 1 s, located mainly in the southwest and eastern Pacific Ocean.

The case of assimilating the wave height only (run 2) is illustrated in Fig. 4a (period of analysis) and Figs. 4b and 4c (period of forecast). The comparison between Figs. 2a,b and 4a,b shows that the spectral information increases the impact of assimilation on wave heights. Furthermore, the decay of the impact with time is faster when only the assimilation of wave height is used, whereas the use of spectral information prolongs the impact. After 2 days of forecast the impact of run 2 on significant wave height is less than 0.1 m, as illustrated in Fig. 4c.

To further analyze the benefit of using spectral information, we computed the assimilation index on the

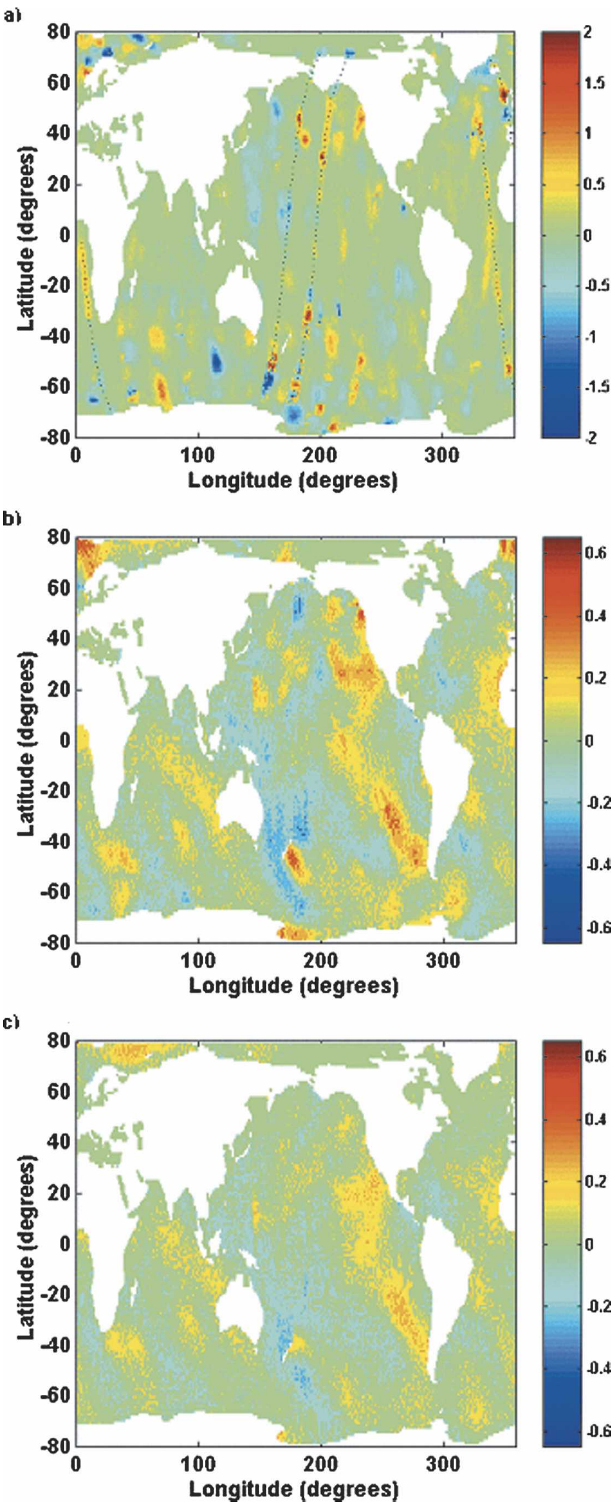

FIG. 2. Difference of significant wave heights (in m) between runs with and without assimilation of synthetic SWIMSAT data (run 1a − run C): (a) 0000 UTC 23 Oct 2000 (after 1 day in the period of analysis) where the dotted lines indicate the location of the synthetic observations for an assimilation time window of 3 h; (b) 0000 UTC 27 Oct 2000 (1 day after the end of assimilation); and (c) 0000 UTC 28 Oct 2000 (2 days after the end of assimilation).

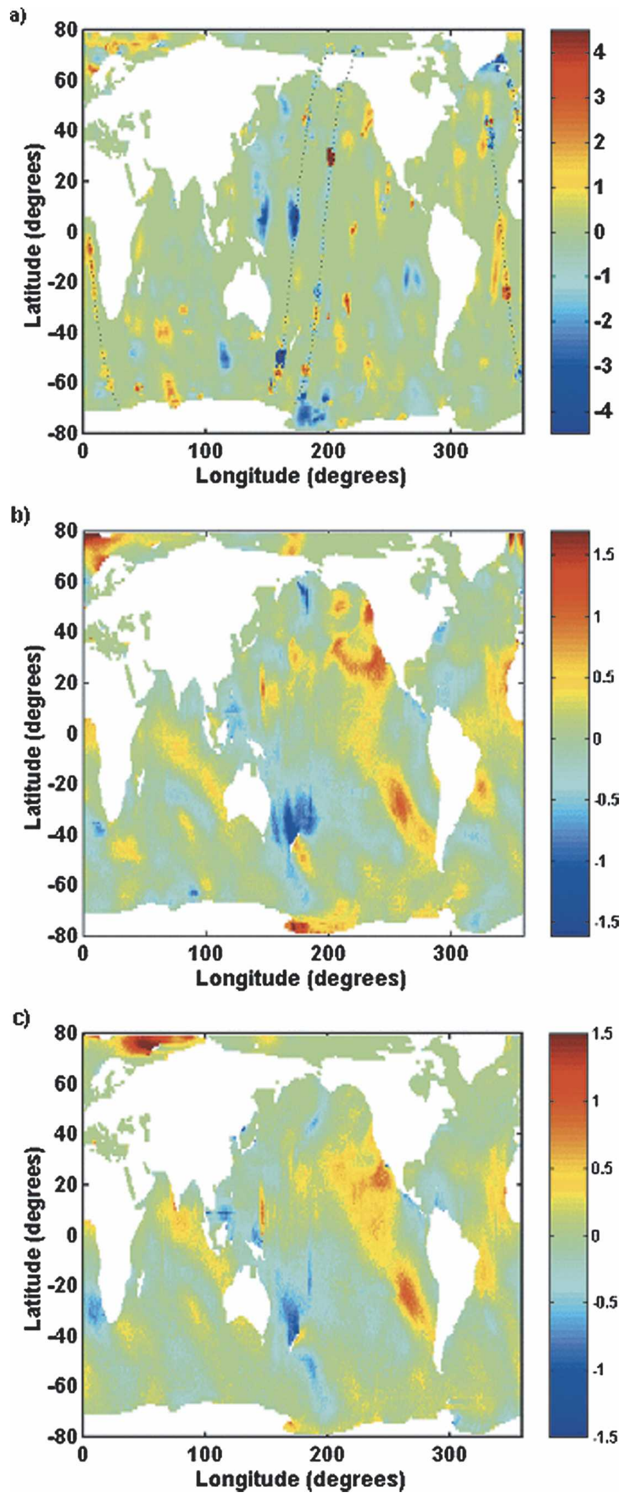

FIG. 3. Difference of mean wave period (in s) between runs with and without assimilation of synthetic SWIMSAT data (run 1a − run C): (a) 0000 UTC 23 Oct 2000 (after 1 day during the period of analysis) where the dotted lines indicate the locations of the synthetic observations for an assimilation time window of 3 h; (b) 0000 UTC 27 Oct 2000 (1 day after the beginning of the period of forecast); and (c) 0000 UTC 28 Oct 2000 (2 days after the end of assimilation).

TABLE 5. Assimilation index of wave parameters during the analysis period (computed at observation locations only) and the correlation coefficient (CC) between modeled and observed wave parameters before and after assimilation. SWH: significant wave height, T_m: mean wave period, θ_m: mean wave direction, and AI: assimilation index.

	SWH		T_m		θ_m	
AI (%)	48.2		28.9		35.6	
	Before	After	Before	After	Before	After
CC	0.88	0.97	0.87	0.94	0.77	0.92

wave parameters over all sea points during the analysis and forecast periods for each case (runs 1a and 2). Figures 5a–d show, respectively, the variation of the assimilation index for significant wave height, low-frequency wave height, mean wave frequency, and direction, during the analysis and forecast periods. The general trend for all these plots indicates that the index increases during the period of analysis until a saturation point; then it decreases progressively during the period of forecast until it becomes very low and tends to 0.

For run 1a (assimilation of spectral information), the maximum index values—calculated here as mean values over all model grid points—occur during the period of analysis and reach 16%, 18%, 17%, and 25% for the significant wave height, mean wave frequency, mean direction, and low-frequency wave height, respectively. The highest index is obtained for the low-frequency wave height; this points out that the assimilation of spectral information is relevant for swell properties. For run 2 (assimilation of wave height only), the assimilation index for significant wave height is similar to case 1a, but the assimilation index for the other parameters (low-frequency wave height, mean wave frequency, mean direction) is significantly smaller than from run 1a.

The difference between the assimilation skills of runs 1a and 2 is more striking for the mean wave direction, where on 24 October 2000 the correction of the rms errors from run 1a is three times higher than the one obtained from run 2, as illustrated in Fig. 5d.

3) Sensitivity to wind perturbation (first guess)

One of the important issues in data assimilation is the specification of the background error. In this section we investigate the use of the first guess from run D, which induces larger standard deviation values on mean wave parameters in comparison with the case of run C [see section 3a(2)]. Thus, the relative errors decrease to 0.2 for significant wave height and 0.4 for wavenumber. Because of the reduced time consumption and with the aim of using the assimilation scheme optimally for run 3, a mean relative error of 0.3 is then used for the computation of a single error covariance matrix. To analyze the performance of the analysis system for different first guesses, we performed a comparison between the results from runs 1a and 3. Figure 6a shows that the assimilation index of significant wave height is larger for run 3 than in the case of run 1a, in particular after the first day of analysis. This clearly indicates that large rms error in the first guess, as in run 3, enhances the assimilation impact with respect to observations. The maximum of the difference between index values of moderate and strong perturbations (first guess) is more than 5%. Furthermore, the impact with respect to observations for run 3 stays efficient longer during the forecast in comparison with the case of run 1a. After a 3-day forecast the assimilation index is still estimated at 2%, while for moderate perturbation (run 1a) the index is completely damped (close to 0) after only a 2-day forecast. The same trend is found for the mean frequency of waves, as illustrated in Fig. 6b. In addition, after the 3-day forecast the impact on mean frequency is still estimated at more than 5%. In agreement with this result, Fig. 7 shows the assimilation impact for significant wave height after a 3-day forecast and it is still estimated at 0.5 m in eastern and intertropical areas of the Pacific Ocean and in southern and eastern regions of the Indian Ocean.

4) Sensitivity to observational errors

The observation error variances are mainly specified according to the knowledge of instrumental characteristics, but they should also include the variance of representativeness errors, which are not negligible when analyzing physical processes and cannot be well described in model space. In this section, a second case of synthetic wave spectra (instrumental error 2 indicated in Table 2) is used to investigate the performance of the analysis system regarding the error increase in the observations. By comparing the error of observations in case 2 (see Table 2) and first guess in case C (see Table 1), the relative errors are approximately estimated at 0.4 for significant wave height and 0.8 for wavenumber. Since we are using a single error covariance matrix to reduce CPU time, we have considered a mean relative error of 0.6 for an optimal run 4. The increase of instrumental errors in synthetic wave spectra is analyzed by comparing run 1a with run 4, which is the case of the assimilation of synthetic wave spectra with a larger error than those used in run 1a (case 2 of the instrumental error in Table 2). Table 6 summarizes the results on the

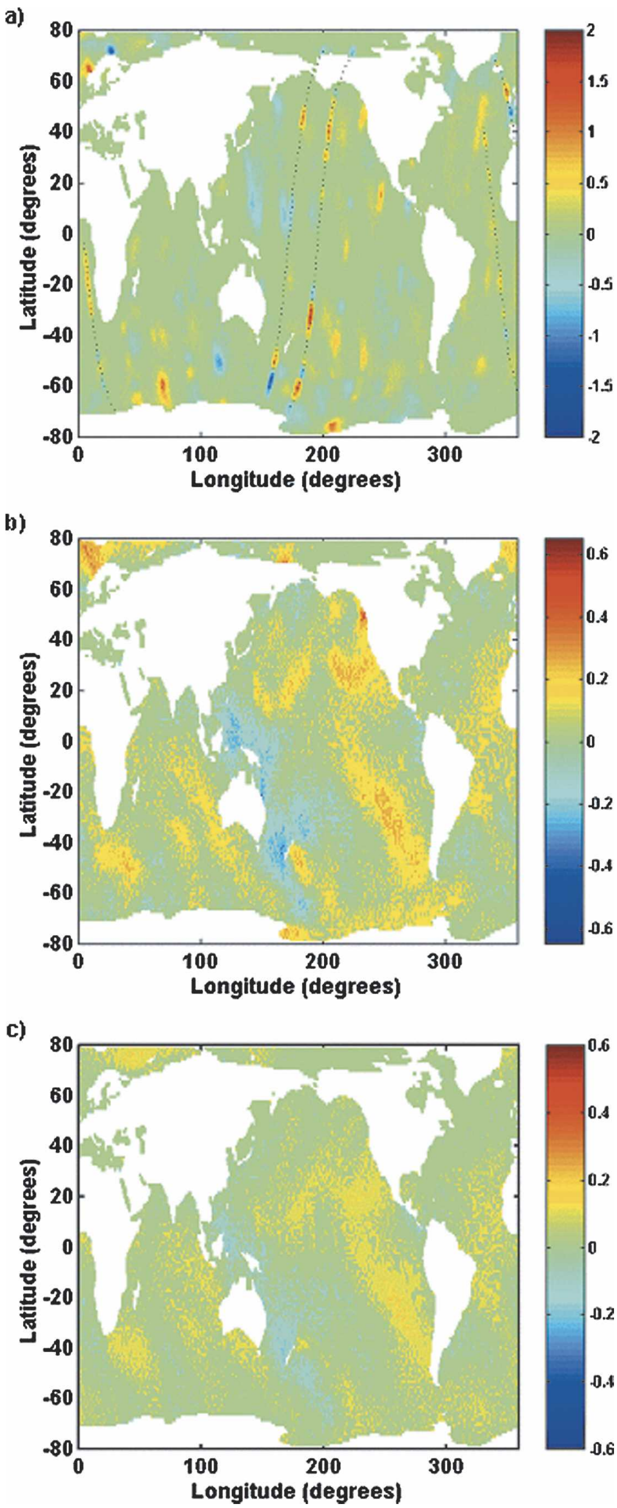

FIG. 4. Difference of significant wave heights (in m) between runs with and without assimilation of wave height only: (a) 0000 UTC 23 Oct 2000 (after 1 day in the period of analysis) where the dotted lines indicate the location of the synthetic observations for an assimilation time window of 3 h, (b) 0000 UTC 27 Oct 2000 (1 day after the end of assimilation), and (c) 0000 UTC 28 Oct 2000 (2 days after the end of assimilation).

average value of assimilation indexes for the periods of analysis and forecast; this concerns significant wave height, mean frequency, and direction of waves. It is clear that the increase in instrumental error induces a decrease in the assimilation index for the mean wave parameters. For the significant wave height the difference is much more pronounced and is estimated at 2% and 0.7% for the periods of analysis and forecast, respectively. For the mean frequency the difference decreases to 1.4% for the period of analysis and 0.3% for the period of forecast. The increase in error for the synthetic observations seems to affect the significant wave height more than the mean frequency. For the mean direction of waves the decrease of the assimilation index when using the instrumental errors of case 2 is about 1.9% and 0.2% for the periods of analysis and forecast, respectively.

In summary, the increase in observation errors has a significant impact on the assimilation index of the mean wave parameters, mainly in the period of analysis (about 1.4%–2%), but this does not change the time evolution of the assimilation index during the periods of analysis and forecast.

5) SENSITIVITY TO CORRELATION LENGTH

The length scale used in the correlation model described by Eq. (3) has a direct effect on the correcting weights in the optimal interpolation. According to Greenslade and Young (2004), the length scale should not be considered as constant since it varies with ocean region. More specifically, it is be more appropriate to use a large length scale for the intertropical region and a small one for high-latitude ocean area. In a previous work (Aouf et al. 2003), we compared the errors of several wave forecasts of the WAM for a global scale and found that the use of a constant correlation length, as in Eq. (3), has a tendency to under(over)estimate the background (forecast) errors, in particular in the intertropical region. To overcome this difficulty we therefore choose a correlation length depending upon the latitudes of observation locations and the effected grid points. Thus, by considering a range of correlation length varying from 150 km for the farther northern and southern latitudes to 350 km for the tropical region, we investigate the use of the following relations in the assimilation scheme:

$$\lambda_i = 350 - 2.4|\Phi_i|, \tag{7}$$

$$\lambda_j = 350 - 2.4|\Phi_j|, \quad \text{and} \tag{8}$$

$$\lambda_c = \sqrt{\lambda_i \lambda_j}, \tag{9}$$

where Φ stands for the latitudes and the subscripts i and

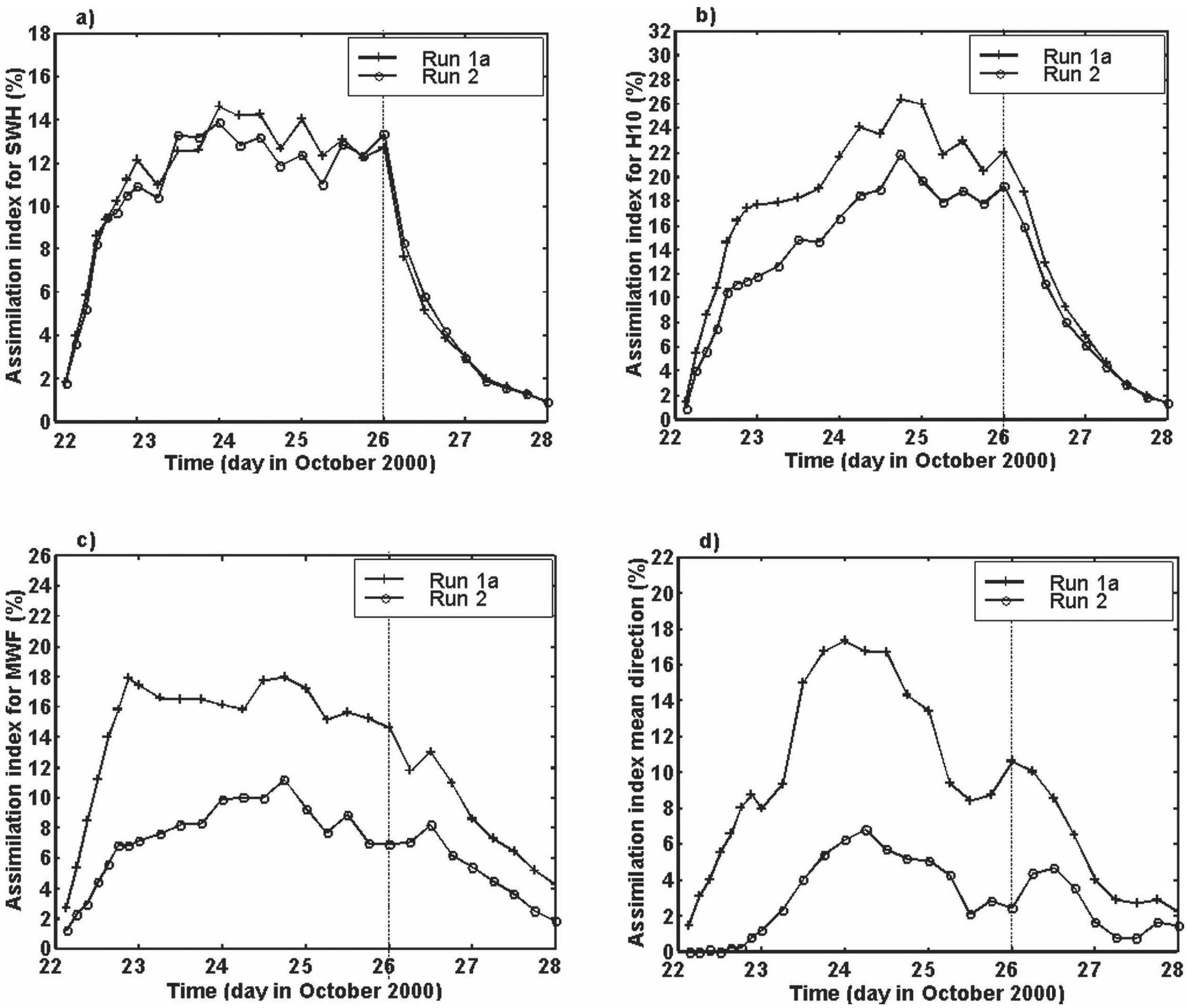

FIG. 5. Time evolution of the assimilation index (computed over all sea points) during the periods of analysis (from 22 until 26 Oct) and forecast (from 26 until 28 Oct). Plus signs and circles stand for the assimilation with spectral information (run 1a) and the assimilation with wave height only (altimeter case run 2), respectively: (a) significant wave height, (b) low-frequency wave height (H_{10}), (c) mean wave frequency, and (d) mean wave direction. The dashed line at 26 Oct 2000 indicates the end of the assimilation period.

j indicate the affected grid point and the observation location, respectively.

We remind the reader that for run 1a we considered a constant correlation length of 250 km, while for run 5 the correlation length is computed from relations (7)–(9). In Figs. 8a and 8b the mean assimilation index for runs 1 and 5 are compared during the periods of analysis and forecast. The use of relation (9) gives better performance for the assimilation scheme during both periods of analysis and forecast. In particular, after the first day of analysis (23 October 2000), the assimilation index for the significant wave height is significantly increased (by more than 2%). During the period of forecast this increase is smaller (about 0.5%).

To further discuss this effect of changing the correlation length, we divided the model domain into three ocean basin regions: namely, intertropical (20°S–20°N), intermediate (20°–50°S and 20°–50°N), and high-latitudes regions (50°–80°S and 50°–80°N). Tables 7a and 7b show the average of the assimilation index for significant wave height and mean frequency of waves, in the periods of analysis and forecast. It is clear that better skill is found for all regions when relation (9) is used for computing the length scale. The improvement is strongest in the intertropical region, where the correlation length is assumed to be larger than the mean. It is of about 2.4% and 1.8% for the significant wave height and the mean frequency of waves in the period of analysis, respectively, and slightly less during the period of forecast. The improvement induced by the re-

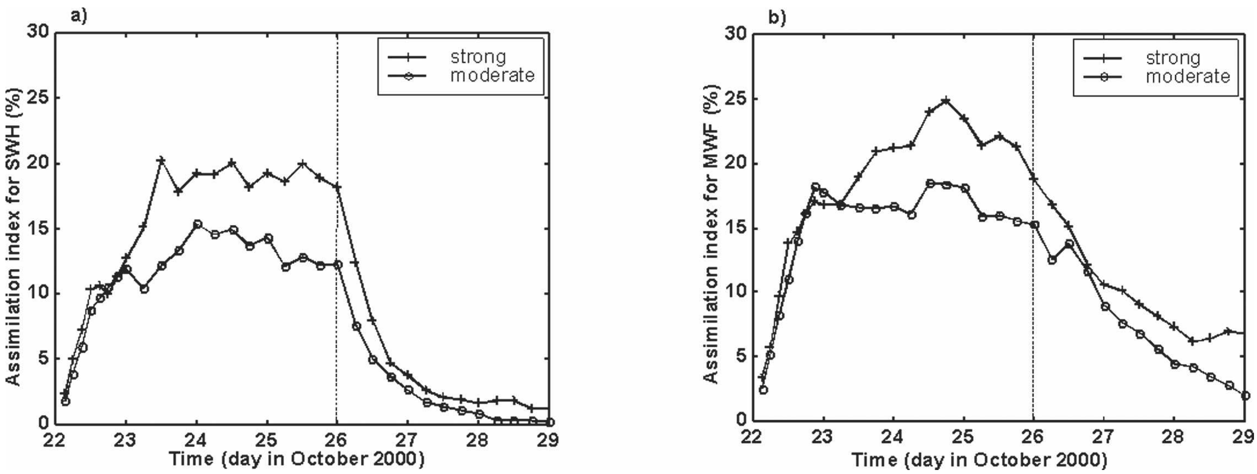

FIG. 6. Time evolution of the assimilation index (computed over all sea points) for moderate (run 1a) and strong (run 3) first-guess perturbations during the periods of analysis and forecast: (a) significant wave height and (b) mean wave frequency. Plus signs and circles stand for strong and moderate first-guess perturbations, respectively. The dashed line at 26 Oct 2000 indicates the end of the assimilation period.

lation (9) is less marked in the intermediate and high-latitude regions, where the difference is less than 1% for both periods of analysis and forecast. For high-latitude regions the use of relation (9) affects the significant wave height more than the mean frequency of waves.

6) SENSITIVITY TO OBSERVED WAVELENGTH CUTOFF

The SWIMSAT radar is expected to provide spectral information for a minimum wavelength of 70 m; this is a real advantage in comparison with the ASAR instrument on board *ENVISAT* (wavelength cutoff of 150–250 m). For this reason, we have adapted the assimilation scheme in order to take into account the wavelength limitation on synthetic wave spectra. More specifically, in this section, assimilation with spectral information at wavelengths longer than a threshold cutoff wavelength is considered. Assimilation runs 6, 7, and 8 are performed for typical wavelengths cutoff of 70, 155, and 240 m, respectively (see Table 3). The results are compared to those obtained from run 1a, which is the case of assimilation without a wavelength cutoff.

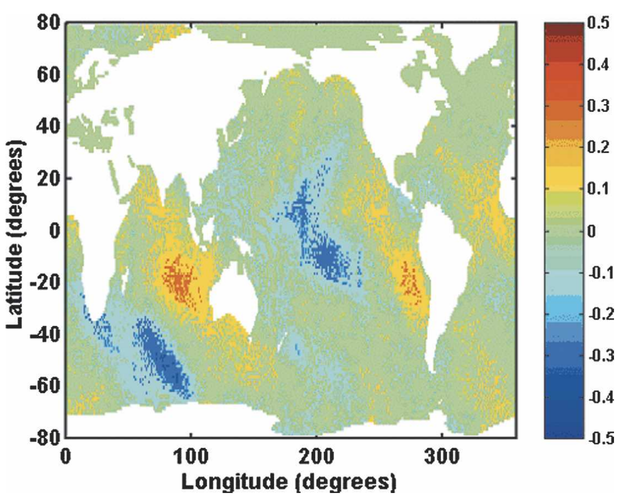

FIG. 7. Difference of significant wave heights (in m) between runs with and without assimilation of synthetic SWIMSAT data in the case of large error on the first guess (run 3 − run D). Output time is 0000 UTC 29 Oct 2000 (3 days after the end of assimilation).

Figures 9a–c show the assimilation index for significant and low-frequency (H_{15}) wave heights, and mean frequency, respectively, from outputs of runs 6, 7, 8, and 1a. For all of these parameters, it is apparent that the increase in wavelength cutoff induces a decrease in the assimilation index. For the significant wave height and during the period of maximum assimilation index

TABLE 6. Influence of the instrumental errors on assimilation results (runs 1a and 4; average value of the assimilation index over all sea points during analysis and forecast periods). AVAI: average value of the assimilation index, SWH: significant wave height, f_m: mean wave frequency, and θ_m: mean wave direction.

	AVAI (%)			
	Analysis		Forecast (2 days)	
	Run 1a	Run 4	Run 1a	Run 4
SWH	12.1	10.1	3.6	2.9
f_m	12.2	10.8	7.8	7.5
θ_m	12.8	10.9	6.1	5.9

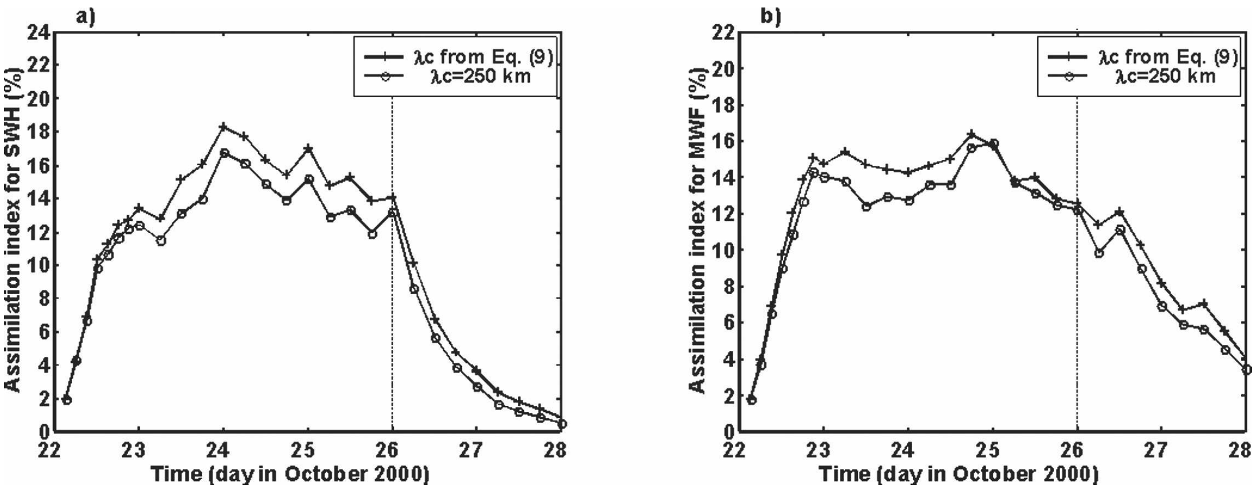

FIG. 8. Time evolution of the assimilation index (computed over all sea points) during the periods of analysis (from 22 until 26 Oct) and forecast (from 22 until 26 Oct) for constant (run 1a) and variable correlation lengths (run 5): (a) significant wave height and (b) mean wave frequency. Circles and plus signs stand for a constant correlation length of 250 km and a correlation length computed from Eq. (9), respectively. The dashed line at 26 Oct 2000 indicates the end of the assimilation period.

(around 24 October 2000), a cutoff wavelength of 70 m exhibits an index value almost 1.6 times greater than that for a 155-m cutoff and 4 times greater than that for a 240-m cutoff wavelength. Correlatively, the assimilation index for low-frequency wave height (H_{15}) decreases from 14% to 10% or 4% when the cutoff wavelength is changed from 70 to 155 m or 240 m, respectively. In comparison, for run 1a, with no wavelength cutoff, the assimilation index for (H_{15}) is about 22% (Fig. 9b). For the mean wave frequency, the difference between assimilation indexes for different wavelength cutoffs is smaller, but still significant. The largest assimilation index is obtained on 25 October with about 20%, 16%, 13.5%, and 6% for the cases with no cutoff and cutoff wavelengths of 70, 155, and 240 m, respectively. The relationship between wavelength cutoff and performance of the assimilation scheme in terms of rms error is well established. This feature suggests that when we increase the wavelength cutoff from 70 to 240 m, we can expect a large decrease (of about 60%) for the assimilation index of the mean frequency.

Such a result is important, in particular for the assimilation of spectral information from different data sources (SWIMSAT and ASAR) or with different surface conditions encountered by SAR, which correspond to different cutoff wavelengths. The outstanding cutoff

TABLE 7. Average value of the assimilation index in different ocean regions during the periods of analysis and forecast. AVAI: average value of the assimilation index, R1: intertropical region (20°S–20°N), R2: intermediate region (20°–50°S and 20°–50°N), and R3: high-latitude region (50°–80°S and 50°–80°N).

	AVAI (%)			
	λc = 250 km		λc from Eq. (9)	
	Analysis	Forecast	Analysis	Forecast
	(a) For significant wave height			
R1	16.3	9.1	18.7	10.9
R2	10.5	1.5	11.4	2.0
R3	12.5	4.0	13.2	4.3
	(b) For mean wave frequency			
R1	13.9	4.9	15.7	6.3
R2	9.1	7.0	9.7	7.6
R3	13.5	8.6	13.8	8.6

AVAI = average value of the assimilation index.
R1 = intertropical region (20°S–20°N).
R2 = intermediate region (20°–50°S and 20°–50°N).
R3 = high-latitude region (50°–80°S and 50°–80°N).

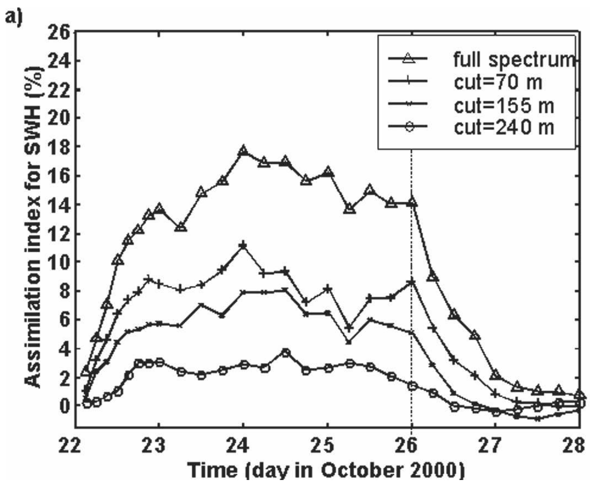

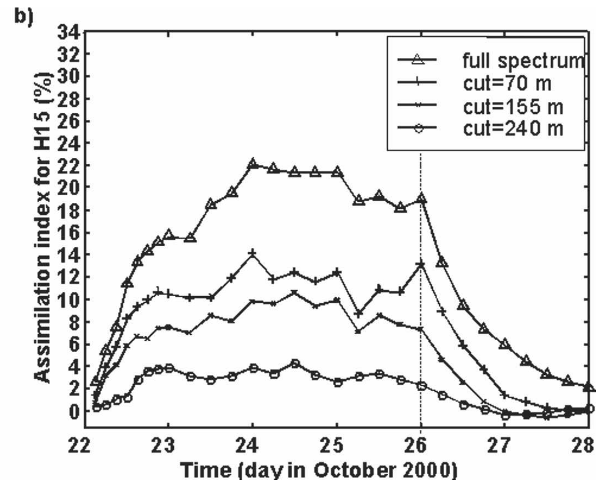

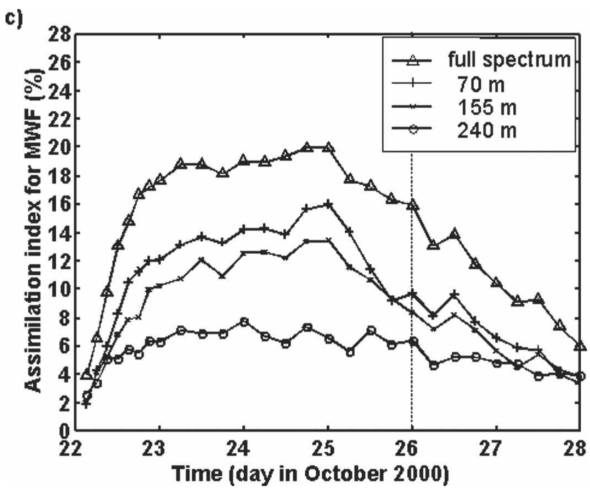

FIG. 9. Time evolution of the assimilation index (computed over all sea points) during the periods of analysis (from 22 until 26 Oct) and forecast (from 26 until 28 Oct) for different wavelength cutoffs, and for (a) significant wave height, (b) low-frequency wave height (H_{15}), and (c) mean frequency of waves. Triangles: with no cutoff, plus signs (+): for a cutoff of 70 m, ×: for a cutoff of 155 m, and o: for a cutoff of 240 m. The dashed line at 26 Oct 2000 indicates the end of the assimilation period.

wavelength in the case of the SWIMSAT data is very promising and guarantees a significant improvement for the estimate of mean wave parameters.

4. Concluding remarks

Algorithms for the assimilation of spectral data in the WAM wave model have been tested successfully and have shown the benefits of using spectral synthetic data, such as those expected from the SWIMSAT satellite. The sensitivity study showed that the correlation model assumed in the assimilation scheme works optimally for two cases: the first case uses a single error covariance matrix with a relative error between background and observation of 0.6 for all wave parameters, while the second case computes separately the error covariance matrix with relative errors of 0.3 for significant wave height and 0.6 for wavenumber. The use of a single error covariance matrix with a relative error of 0.6 is preferred because it is less time consuming.

The simulations emphasized the need for keeping the error of observations as small as possible. Their increase reduces significantly the assimilation index of the mean wave parameters, in particular during the period of analysis. But accounting for realistic observations, the error does not dramatically change the assimilation impact.

It was shown that the assimilation impact, with respect to the "no assimilation" case, is significant during the analysis, and is reliable for a 2-day forecast with moderate errors in the first guess. In addition, larger errors in the first guess enhance the assimilation impact; with respect to the no assimilation case it is significant for up to a 3-day forecast, for a first-guess error that remains realistic.

It has been shown that the assimilation of spectral information provides better skills for both periods of analysis and forecast, in comparison with the assimilation of wave height only. This result is more pronounced for low-frequency wave height (H_{10}), mean frequency, and direction of waves than for the standard total significant wave height. Furthermore, when spectral information is used, the assimilation impact with respect to observations is more prolonged for the period of forecast than for the case of assimilation of wave height only.

Using a correlation length depending on latitude, as proposed in Eq. (9), leads to a better spread of the incremental observations and consequently gives better performance in terms of rms errors.

Accounting for a cutoff wavelength due to limitations in the observations induces a reduction of the assimilation index for the mean wave parameters. For a 70-m wavelength cutoff, as expected for SWIMSAT data, the decrease of performance with respect to a perfect case without a cutoff is relatively small, and the impact is still relevant. However, for a large wavelength cutoff of 240 m, as often expected from SAR systems, the impact of assimilation is very small on all wave parameters. For an intermediate cutoff value (155 m), the impact is close to (although weaker than) that obtained for the 70-m cutoff.

In the context of future work, we will investigate a better description of the correlation model on a global scale. For this matter, the distribution of background error could be computed by comparing long wave period wave forecasts from the WAM with the wave observations from altimeters (Greenslade and Young 2004).

The assimilation system is in preparation for operational use and we have already started to validate and assimilate "real" spectral wave data obtained from the ASAR level 2 wave products of *ENVISAT*. In this case, a combination of assimilation of wave height only from the altimeter data and of spectral data from ASAR will be implemented. The assimilation schemes are implemented separately since the two observations are not collocated (separation of about 200 km across track of the satellite). In future work, it will be necessary to optimize the combination of these two assimilation schemes. In addition, a study with the combination of several spectral data sources should be carried out in order to establish the complementary contribution of each data source. Also, long periods of assimilation with real data are needed to evaluate the assimilation impact with respect to independent wave data such as those obtained from buoys and altimeters.

Acknowledgments. The authors thank Eric Thouvenot for providing the orbit track data for SWIMSAT. In addition, we gratefully acknowledge support from the French space agency (CNES). We also would like to thank the anonymous reviewers for their valuable comments.

APPENDIX A

Low-Frequency Wave Height

Low-frequency swell height is defined as the wave height computed for a limited frequency band of the wave spectrum. This can be obtained from the following relation:

$$H_{10} = 4\sqrt{\int_{f_1}^{f_{10}} E(f)\,df}, \tag{A1}$$

where $E(f)$ is the density of wave energy, while f_1 and f_{10} are the first value in the frequency interval of the wave spectrum ($f_1 = 0.044$ Hz) and the cutoff frequency ($f_{10} = 0.1$ Hz). For the low-frequency wave height H_{15}, the relation (A1) is computed with a frequency cutoff (f_{15}) of 0.15 Hz, instead of f_{10}.

APPENDIX B

Assimilation Index

The assimilation index describes the skill of the assimilation scheme. This parameter indicates the percentage of correction on the rms error of the wave parameters:

$$\mathrm{AI} = \frac{\mathrm{RMSN} - \mathrm{RMSA}}{\mathrm{RMSN}} 100(\%), \tag{B1}$$

where RMSN is the root-mean square of the difference between the synthetic observed wave parameters and the wave parameters obtained without assimilation while RMSA is the root-mean square of the difference between the synthetic observed wave parameters and the wave parameters obtained with assimilation. The closer to 100% the index value is, the closer to the observations the analyzed wave parameters are and, thus, the better the assimilation skill is. On the contrary, a negative index value means that the assimilation degrades the first guess.

REFERENCES

Aouf, L., J. M. Lefèvre, and D. Hauser, 2003: Optimization of the assimilation scheme of directional wave spectra in wave model WAM: Application to real ASAR ENVISAT wave spectra. *Proc. Int. Society for Off-shore and Polar Engineering (ISOPE) Conf.*, Kita-Kyushu, Japan, 106–112.

Bidlot, J. R., D. J. Holmes, P. A. Wittmann, R. Lalbeharry, and H. S. Chen, 2000: Intercomparison of the performance of operational ocean wave forecasting systems with buoy data. ECMWF Tech. Memo. 315, 46 pp.

Breivik, L.-A., M. Reistad, H. Schyberg, J. Sunde, H. E. Krogstad, and H. Johnsen, 1998: Assimilation of ERS SAR wave spectra in an operational wave model. *J. Geophys. Res.,* **103,** 7887–7900.

Dunlap, E. M., R. B. Olsen, L. Wilson, S. De Margerie, and R. Lalbeharry, 1998: The effect of assimilating *ERS-1* fast delivery wave data into the North Atlantic WAM model. *J. Geophys. Res.,* **103,** 7901–7915.

Greenslade, D. J. M., and I. R. Young, 2004: Background errors in a global wave model determined from altimeter data. *J. Geophys. Res.*, **109,** C09007, doi:10.1029/2004JC002324.

Günther, H., and Coauthors, 1992: Implementation of a third generation ocean wave model at the European Centre for Medium Range Weather Forecasts. Final Rep. for EC Contract SC1-0013-C(GDF), ECMWF, Reading, United Kingdom, 34 pp.

Hasselmann, S., C. Brüning, K. Hasselmann, and P. Heimbach, 1996: An improved algorithm for the retrieval of ocean wave spectra from synthetic aperture image spectra. *J. Geophys. Res.,* **101,** 16 615–16 629.

——, P. Lionello, and K. Hasselmann, 1997: An optimal interpolation scheme for the assimilation of spectral wave data. *J. Geophys. Res.,* **102,** 15 823–15 836.

Hauser, D., L. Aouf, and J.-M. Lefèvre, 2001a: Prospect of new ocean waves spectral observations from the SWIMSAT satellite: Measurements and assimilation. *Proc. ECMWF Workshop on Ocean Wave Forecasting,* ECMWF, Reading, United Kingdom, 135–145.

——, E. Soussi, E. Thouvenot, and L. Rey, 2001b: SWIMSAT: A real aperture radar to measure directional spectra of ocean waves from space: Main characteristics and performance simulation. *J. Atmos. Oceanic Technol.,* **18,** 421–437.

Kalnay, E., 2002: *Atmospheric Modeling Data Assimilation and Predictability.* Cambridge University Press, 341 pp.

Komen, G. J., L. Cavaleri, M. Donelan, K. Hasselmann, S. Hasselmann, and P. A. E. M. Janssen, 1994: *Dynamics and Modeling of Ocean Waves.* Cambridge University Press, 532 pp.

Le Meur, D., J.-M. Lefèvre, H. Roquet, and J. Tournadre, 1995: Apport des capteurs actifs micro-onde d'ERS-1 et de TOPEX/POSEIDON à la modélisation numérique des vagues. *Act. Atelier Modél. Atmos.,* **1,** 83–89.

Lionello, P., H. Günther, and P. A. E. M. Janssen, 1992: Assimilation of altimeter data in a global third-generation model. *J. Geophys. Res.,* **97,** 14 453–14 474.

Voorrips, A. C., V. K. Makin, and S. Hasselmann, 1997: Assimilation of wave spectra from pitch-and-roll buoys in a North Sea wave model. *J. Geophys. Res.,* **102,** 5829–5849.